Operator training for distant interactions with EEG and EIS based feedback

S.Kernbach[1], V.Zhigalov[2], A.Fedorenko[3], J.Pfeiffer[4], G. Peng[5], O.Kernbach[1], A.Kernbach[1], E.Gorokhov[6]

***Abstract*—This paper reports on distant consciousness-device experiments performed as a long-range signal transmission between spatially separated human-'transmitters' and device-'receivers'. These experiments have been conducted between 2015 and 2019 with operators from the USA, Canada, Europe, Russia, China and Argentina. Signals on the receiver side are detected by electrochemical impedance spectroscopy (EIS) of aqueous solutions. They are displayed as real-time html plots streamed in internet and represent a remote feedback. Local feedback is provided by EEG data available for operators also in real time. Distance between operators and EIS devices varies between 10^1 to 10^6 meters. Combination of remote EIS and local EEG feedbacks enables controllable conditions for operators and contributes to achieving well-repeatable outcomes. Experiments demonstrated initial 74% of success in web-based attempts that is improved up to 96%-98% with increasing the number of repeating attempts. Authors express a hypothesis towards quantum nature of such experiments that are generated and measured on a macroscopic level by biological and technological systems. The developed approach has multiple applications, this paper considers its usage for training of operators who target distant activities.**

I. Introduction

The long-range signal transmission experiments started in 60s and 70s of XX century in different fields of biophysics, instrumental psychotronics and military applications that later resulted in quantum-mind research of 90s. There are well-known experiments with human operators (transmission of visual information on distances of several hundred km) organized by Vasiliev [1], animals (analysis of EEG data of twin rabbits on the distance of 22 km) performed by Perov [2], Akimov's experiments with plants [3], 'remote action' experiments by Hubbard [4], military research of USSR and USA [5]. In XXI century these experiments are essentially improved by the distance (up to 13750 km) [6], by used devices and by the methodology of performed attempts. Significant statistics has been collected both for the number of replications and for diversity of used instruments and operators.

The main idea of these experiments consists in observation that electrochemical processes, expressed in the form of ionic dynamics, are sensitive to non-contact 'weak impact-factors' generated by various entropic, electromagnetic or even mechanical processes [7]. The high-resolution AC/DC conductometry and EIS spectroscopy have become popular methods for analyzing such weak phenomena. There are several variants of corresponding methods/devices, such as measuring the relative dispersion of conductivity [8], analyzing the DC-current-conductivity [9], [7], detector on deeply polarized electrodes [10], contactless measurement of conductivity [11] and differential EIS [12]. Conductometric systems were used for testing human operators, for example, the two-channel system developed by Dr. Bobrov in 80s and 90s [13]. The fact of involving the 'consciousness-consciousness' and 'consciousness-device' approaches into different governmental programs was emphasized in numerous interviews and publications [14], [15], [5]. Current journal publications [16], [17] point to a possible intensification of these works.

Similar effects have been studied in different countries. For example, large-scale studies of External Qi, especially for its distant form, have been conducted in China. Many Qigong Masters had the ability of remote healing. The most famous case was the cooperation of Yan Xin, Tsing Hua University and Institute of High Energy Physics in Beijing. The research results include the influence of Qigong External Qi on the molecular stricture of materials at the distance of 2000 kilometers [18], on the laser polarization plane [19], on aqueous solutions measured by Laser Raman spectroscopy [20]. It was found that the effect of Qigong External Qi was almost the same at the distance of 7 and 2000 kilometers. This effect is assumed to be related to a macroscopic entanglement [21], [22], [23], [24], [25].

This paper describes public experiments performed during 2015–2019 on the transmission of distant impact on electrochemical test systems with human operators and technical/hybrid devices located in the USA, Canada, Europe, Russia, China and Argentina. The experimental data from sensors are transmitted as html graphs in internet in real time, which create a remote feedback loop between the 'transmitter' and 'receiver'. These experiments are performed as an 'open science approach' using web platforms (for example, aquapsy.com). Various applications of this system for emergency signalling or remote monitoring have already been described e.g. in [6], [26], here we focus on operator training applications.

The studies [27], [28], [29] demonstrated training of mental abilities of operators for deep meditation, stress reduction, psychosomatic regulatory functions, in sports and for use in the brain-computer interfaces (BCI). The papers [30], [31], [32] report on gifted people and the necessity of operator selection for extrasensory perception (ESP), but also stress that the ESP capabilities can be significantly improved through systematic training. A similar experience has been gained in

[1]Cybertronica Research, Research Center of Advanced Robotics and Environmental Science, Melunerstr. 40, 70569 Stuttgart, Germany, Contact author: serge.kernbach@cybertronica.de.com;[2]NRU Moscow Institute of Electronic Technology, zhigalov@gmail.com; [3]Nu-tech, Canada, faa@phystech.edu; [4]Independent researcher, USA, SVP Water Research, 369@svpwaterresearch.com; [5]Ennova Health Science and Technology Co., Ltd., ENN Group, Langfang, Hebei 065001, China, gpufo@outlook.com; [6]Independent researcher, Argentina, gorokhove@gmail.com

Buddhist temples (for example, the Wat Phra Dhammakaya temple in Thailand and its branches in Nepal and Germany) that practice various forms of meditation. Lucid dreaming can also be improved through systematic training [33], similar data are found for teaching healers [34]. However, traditional methods of mental training do not have objective feedback; this leads to a long-term trial and error process. The introduction of neurocognitive feedback based on EEG (for example, using commercially available devices MUSE, EMOTIV, NeuroSky, and others) reduces the training time and improves its quality [35]. An interesting aspect of this study is collective neurocognitive feedback and BCI for large audiences [36].

Experiments with remote EIS-based feedback indicated a similar trainability also for 'non-local skills'. We understand here primarily the operator's capability of distant interactions, e.g. distant healing, remote impact on biological and water-containing systems, or interactions with symbolic objects. Initial web-based experiments demonstrated about 74% of positive outcomes in remote EIS attempts, operators achieve about 96-98% success rate after systematic training. Moreover, the combination of local EEG and remote EIS feedback allows operators to correlate certain altered states of consciousness (for example, special visualization methods) with targeted 'remote actions'. Collective distant attempts, during e.g. collective meditation [37] or joint sessions with several operators [6], are of especial interest. The EEG/EIS method contributes to a deeper understanding of synchronization processes and how collective efforts influence the overall result.

From a scientific point of view, the combination of EEG and EIS approaches enables investigating individual and collective neuro-cognitive processes during such 'non-local tasks'. For example, there is a predominance of alpha rhythm with flat delta and theta dynamics during relaxation and meditation exercises, which correspond to the published results. However, when the operator switches to the 'non-local mode', alpha, delta and theta rhythms significantly increase their intensity, moreover, the delta and theta rhythms generate high intensity waves that approach and even exceed the alpha level. In some cases, the beta rhythm is included in such waves, which indicates the role of visualization processes in these tasks. Asymmetry of the left/right and front/rear data channels is also observed. In general, EEG data allow expressing a hypothesis that 'non-local activities' differ from relaxation or deep meditation practices and require a special approach for their training.

This work is organized as follows: sections II and III describe the equipment, setups and methodology. The section IV overviews non-local experiments with and without local EEG feedback and with different EIS setups. Finally, the section V concludes this work.

II. Setup and experimental methodology

Experiments in this work use the electrochemical impedance spectrometer with optical excitation [12], see Fig. 1, and the commercially available MUSE-2 EEG sensor. The EIS system is capable of performing high-resolution differential measurements, to increase their accuracy, the system is thermally stabilized at the level of the printed circuit board and liquid samples

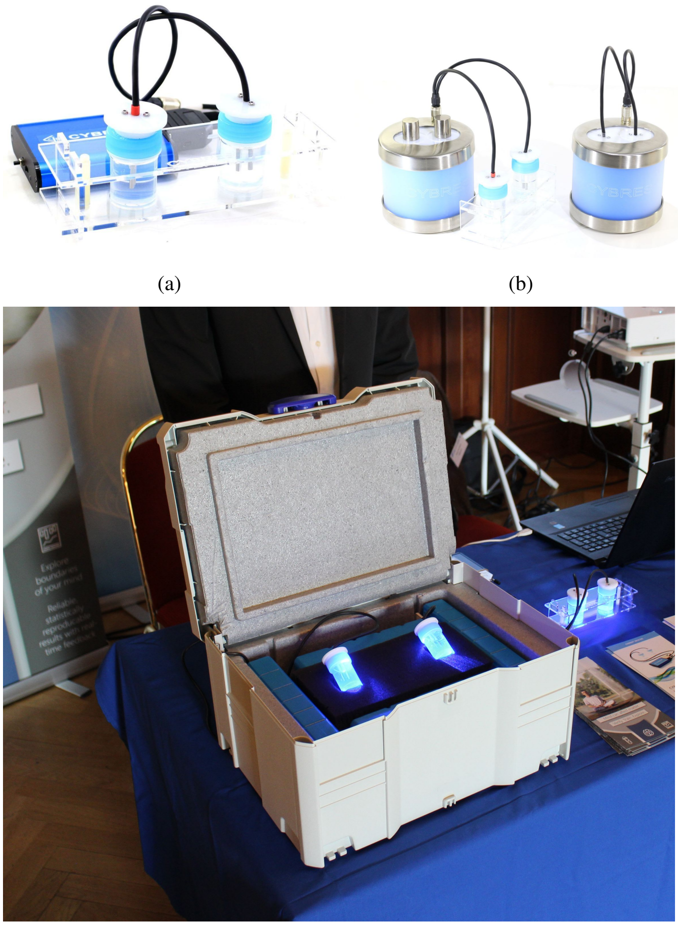

(a) (b) (c)

Figure 1. CYBRES EIS differential impedance spectrometer, versions with **(a)** open electrodes and optical excitation; **(b)** thermostating fluid samples; **(c)** a thermostabilized neopor container and thermo-compensating gel inside (exhibition 'Complementary Medicine 2019', Heidelberg, Germany), trademarked as the M.I.N.D. system.

(in the version with thermostat, see Fig. 1(b)). The EIS spectrometer records up to 60 data channels from electrochemical, thermochemical and external sensors, statistical and numerical calculations. The main applications are characterization of non-chemical treatment of fluids, detection of weak electrochemical changes caused by external factors, water handling, infoceutical production and other similar measurements. The entire system and its individual aspects were published in [38], [39], [40], [41], [12] and others. An example of such a system with thermo-insulated container is shown in Fig. 1(c).

Since these experiments deal with weak signals, all setups are installed in basement/separate rooms with stable environmental conditions, without sunlight, mechanical influences or electrical devices generating strong electromagnetic fields near the sensors. To collect data and calculate statistical parameters, a statistical server was used that also transmitted html data of real-time plots in the Internet. The environmental conditions are continuously recorded: the temperature at 6 points in each device, RF radiation 0.45-2.5 GHz, supply voltage, air pressure, 3D accelerometer and magnetometer. Correlations of electrochemical data with data from these sensors are monitored during active sessions to exclude influence of local environmental conditions on experimental results, see [42].

Experimental methodology. Early experiments (before 2015) are published in [43], [6], all attempts between 2015 and 2019 are divided into early web-based setups (2015-2017) with manual processing of results, and the setup with automated analysis (2018-2019). The general methodology of early experiments is described in [44]. Synchronization of attempts, assignment of sensors and discussions of results took place publicly in internet forums, different approaches with online graphs or images were used for targeting remote sensors. The distance between operators and sensors ranged from 3 km to 12000 km (based on google maps), an overview of 39 attempts in September-January 2016-2017 is given in Table II.

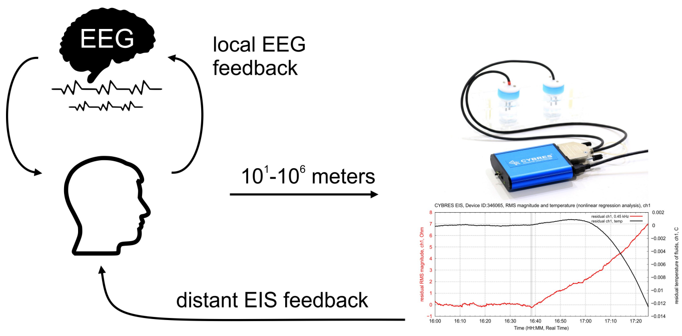

Figure 2. Two real-time feedback loops in experiments 2018-2019: local EEG and distant EIS feedback.

In the sessions 2018-2019, instead of many different operators, a systematic training was conducted within small homogeneous groups (2-5 operators) with real-time bio-feedback, consisting of two feedback loops, see Fig. 2. The local feedback was provided by EEG sensors, and the distant feedback – by EIS devices. Training sessions were organized along different tasks with increasing complexity: from focusing attention up to intentional increasing or decreasing the trend of electrochemical reactions. Involving EEG-based feedback allowed operators to correlate their mental states with the outcomes of distant attempts, and thus achieving better results, see more in Sec. IV-A. Several sessions in 2019 have been performed with Reiki methodology, see Sec. IV, their systematic analysis is published in [45]. In all attempts 2018-2019, operators had 10-20 minutes for preparations, and 30 minutes for active sessions. The training was performed mostly in the morning time or twice per day (morning and evening sessions). Results of 90 different control and 90 experimental sessions are shown in Table I, their detailed analysis – in Figs. 6–9.

III. Automated EIS data analysis

Automated data analysis represents an important step of experimental methodology that enables two advanced functionalities. Firstly, it allows long-term autonomous operations of measurement system. Passive sessions without influences from operators are analyzed in the same way as active sessions – this is suitable for a long-term analysis of weak environmental fluctuations, e.g. from global events. Data from electrochemical and secondary sensors are compared for tracking of artifacts. Secondly, since conducting of experiments at the receiving side and analysis of sensor data do not involve human persons, this allows avoiding different operator effects and biases in EIS attempts.

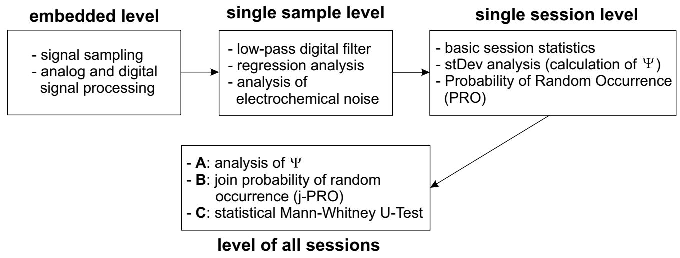

Figure 3. EIS data processing at four levels: in the device (embedded), at the levels of single samples and single sessions, as well as on the level of all sessions.

EIS data processing occurs at four levels: in the device (embedded), at the level of single samples and single sessions, see Fig. 3. The last level of all sessions involve statistic processing in blocks of 30 attempts. This level distinguishes *'active experimental sessions'* and *'passive sessions without operators'*. As mentioned, experimental and control blocks are automatically analyzed by the same algorithm, thus passive sessions represent the control experiments. Sampling of all data requires about 70 ms, for noise reduction they are averaged in the embedded level within 30 samples and provided to the application software as 1 sample (up to 60 data channels from different sensors) per second.

A. *Analysis on the session level*

The regression and stDev analysis. The dynamics of EIS data is divided into two phases: the phase B – background recording (time prior to a session); the E phase is an experiment (or a session). Impact identification is based on the difference of EIS dynamics in the B and E phases, see Fig. 4 – external influence disturbs the EIS dynamics in the E phase. The main goal of regression analysis is to assess the difference between *expected dynamics* based on approximated data from B region and the *observed dynamics* in the E region, perturbed by 'impact factors'. If there are no differences, it means there are no 'impact factors', otherwise deviations from the expected dynamics allow identifying these factors.

The original data $data(x)$ in the background region B from EIS devices is approximated linearly

$$fit_L(x) = a_l x + b_l, \tag{1}$$

or by the nonlinear function

$$fit_N(x) = a_n x^5 + b_n x^4 + c_n x^3 + d_n x^2 + e_n x + f_n \tag{2}$$

using the Levenberg-Marquardt algorithm [46], where we consider the residual curve

$$res(x) = fit_{L,N}(x) - data(x). \tag{3}$$

The $res(x)$ function is shown on all regression analysis charts, see Fig. 4. The function $fit_N(x)$ shows better results than $fit_L(x)$, and behaves more sensitive to small perturbations.

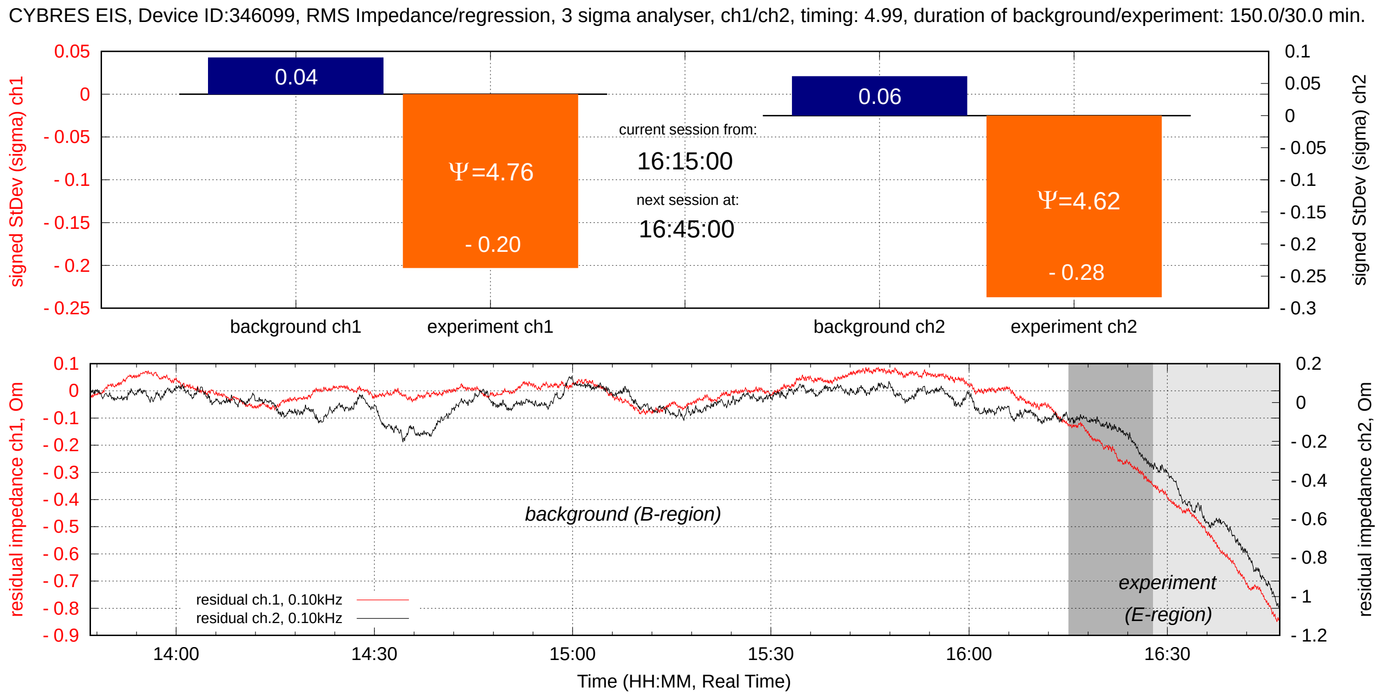

Figure 4. Example of graphical output: (upper graph) bar graphs represent standard deviations in the background and experimental regions of channels 1/2 and '3 sigma rules', the corresponding experimental graph turns orange with a significant change in $\Psi > 3$ and' experimental Ψ '>' averaged Ψ '; (lower graph) residual dynamics of both channels after regression analysis. The gray bar indicates progress of the session.

The optimal time for regression is approximately 3x (background recording is 3 times longer than the experiment), a shorter time does not provide a sufficient number of samples. Thus, 30 minutes of an experiment require about 90-120 minutes of background recording. When the influence on E within the active session is completed, the 'old E region' is shifted to the background and the regression starts again.

Disturbances are expressed as statistical values – as standard deviations σ; σ_B characterizes the background, σ_E characterizes the experiment. The ratio

$$\Psi = k\frac{\sigma_E}{\sigma_B} \tag{4}$$

represents the numerical result Ψ: the more intense are perturbations in the region E, the higher are the values of Ψ. The coefficient k reflects the downward or upward trend, $k = -1$ if EIS dynamics goes down in the E phase (less than zero) and $k = 1$ – otherwise. Each EIS sensor has 2 independent channels, both can be used for experiments.

The probability of Ψ as a random event. The result Ψ is considered to be significant if the EIS dynamics is *qualitatively different* in the areas of B and E. There are two ways for automatic calculation of such a *qualitative difference*: by comparing mean and standard deviation of the EIS data (μ and σ), and by calculating the probability of random occurrence of Ψ scores.

For the first approach, the mean and standard deviation are calculated separately for the regions B and E as μ_B, σ_B and μ_E, σ_E. Applying the '3 sigma rule', B and E are *qualitatively different* if

$$\Psi = \frac{\sigma_E}{\sigma_B} \geq 3. \tag{5}$$

However, two effects influence (5): the nonlinearity of regression and environmental/sensor fluctuations. It was noticed that critical values of $\frac{\sigma_E}{\sigma_B}$ depend on Ψ_{mean}, calculated from 48 or 96 previous sessions. In fact Ψ_{mean} indicates the measurement mode of the sensor and the level of environmental fluctuations.

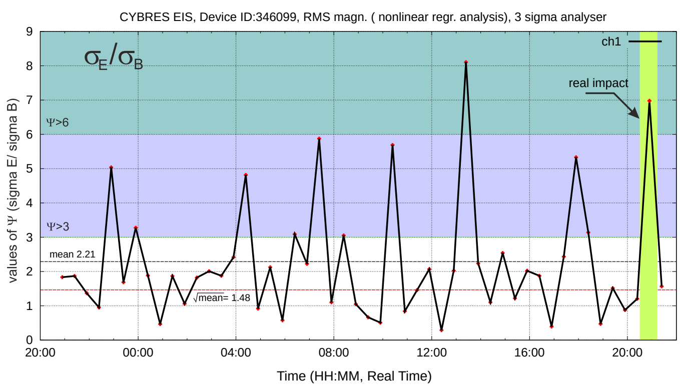

Figure 5. Examples of Ψ calculated every 30 minutes for 24 hours in passive sessions (no experiments). The last two results represent active sessions (an experiment on remote influence on the sensor).

In order to make critical values of Ψ more adaptive to sensors/environment, it makes sense to compare Ψ and Ψ_{mean}

$$\frac{\Psi}{\Psi_{mean}} \geq n, \tag{6}$$

where n is a numerical factor. The expression (6) is an adaptive variant of (5), but for estimating critical values of n it needs to know the frequency of occurrence of Ψ in past sessions. The example of Ψ from real EIS sensor recorded for 24 hours is shown in Fig. 5. For these values, the Probability of Random Occurrence (PRO) can be calculated, e.g. $\Psi > 6$ has 1/48 = 0.0208, $\Psi > 5$ – 5/48 = 0.1041, $\Psi > 3$ – 10/48 = 0.2083, $\Psi > \Psi_{mean}$ – 13/48 = 0.2708. A real remote experiment yields $\Psi = 6.97$, which has PRO of 0.0208. Thus, the value of Ψ, which *is obtained during the experiment*, can be calibrated by PRO. The lower the PRO is, the less likely Ψ represents a random noise.

B. Analysis on the level of all sessions

The sensor constantly takes measurements in sessions of 30 minutes and calculates Ψ and PRO values. Results are accumulated in the table of all sessions for last 24 or 48 hours. Operator can made the sessions active, Ψ and PRO from them are accumulated in the table of active sessions. Due to regression analysis, the effect created by the operator can appear first during the next session. To register such results, two sessions after the active one are considered as 'secondary-active' (post-sessions). If Ψ in post-sessions are higher than in the active session, they are also considered as the result and are entered into the table of active sessions. As soon as the number of experimental attempts reached the specified quota (e.g. 93.75% as 30 attempts from 32), the table of 30 active sessions is analyzed and characterized by the following three factors A, B, and C:

1. Factor A: Numerical assessment of results. Since individual sessions are held in different operator/sensor/environmental conditions, it is necessary to evaluate all active sessions for a general numeric assessment. The table of results has two the current mean Ψ_{mean} and Ψ of active sessions. For N performed active sessions, the following value

$$A = \frac{1}{N} \sum_{N} \left(\frac{\Psi_i}{(\Psi_{mean})_i} \right) \tag{7}$$

provides a numerical characterization of active sessions absolved by the user.

2. Factor B: Joint Probability of Random Occurrence (jPRO). The joint probability jPRO can be calculated by multiplying PROs from active sessions. For example, if $PRO_1 = 0.2$ and $PRO_2 = 0.1$, their product is $jPRO = PRO_1 * PRO_2 = 0.02$. In other words, performing several positive experiments can significantly improve the probabilistic estimates of experimental sessions. To obtain an estimate of the factor B, jPRO must be compared with the 'standard random' sequence in which PRO=0.5

$$B = \frac{\prod_N PRO}{\prod_N 0.5}. \tag{8}$$

The choice of PRO=0.5 is motivated by the average values of Ψ. If active sessions are close to average (random), then the factor $B \geq 1$. The smaller the factor B, the more active sessions differ from random ones in terms of the joint probability of independent events.

3. Factor C: Statistical difference between active and random sessions. The factor B estimates the difference in the joint probability of active and random sessions, but it does not provide clear criteria for assessing a statistical difference between these sessions. For this, the nonparametric Mann-Whitney U-test is used, where the 'null hypothesis' – active sessions are random. The null hypothesis is rejected if the test result is below critical (with 1% and 5% error). The calculation uses the rank sums of all Ψ and Ψ_{mean}

$$C = N^2 + \frac{N(N+1)}{2} - T, \tag{9}$$

where T is the largest of the rank sums (Ψ or Ψ_{mean}).

The results of B and C (j-PRO and U-test) allow estimating the randomness of active sessions. The A and B are important for user's self-assessment, they show the level of his/her abilities and the progress of training. The factors A, B, and C are also calculated to 30 values in the table of all sessions, which can be used as control attempts or for monitoring purposes.

IV. Experimental Results

Summary of 39 attempts from September-January 2016-2017 is given in Table II, the Table I contains overview of 90 experimental results between May and November 2019 with detailed analysis shown in Figs. 6, 7, 9.

Table I
VALUES OF FACTORS A, B, AND C IN DIFFERENT CASES, SEE FIGS. 7, 9, EACH CASE HAS 30 ATTEMPTS.

factor	simul. random (RNG)	real random (EIS)	maximal (EIS)	public June 2019	public Septem. 2019	Reiki Oct. 2019
A	1.04	1.04	2.36	1.96	1.91	2.27
B	2.64^{4}	9.55^{-2}	2.82^{-26}	4.12^{-20}	4.82^{-19}	1.6^{-21}
C	445	422	0	12	80	54

We observe a variation of the factor A between 1 and 2.4, the factor B – between 10^4 and 10^{-26}. The Mann-Whitney test did not reject the null hypothesis for any control (random) data, however the null hypothesis was rejected for the *maximal* case and all *real sessions*.

Assessing boundary cases A, B, C in control attempts. Table I contains A, B, C parameters for several control cases: *simulated random* – the random number generator (instead of the real EIS device) provides input data to the algorithm; *real random* – the table of all sessions from a real EIS device without active sessions; *maximum* – using a real EIS device, where the table of active sessions contains 30 maximal values sorted from all sessions within 3 days, Fig. 6 shows the original data for this case.

Example of web-based sessions 2016-2017. These experiments correspond to early stages of development, where the result was estimated by a significant deviation of trend and the Ψ value was not calculated. The general methodology of those experiments is described in [44], an overview of September-January 2016-2017 attempts is given in Table II.

Successful or unsuccessful attempts are registered only in methodologically correct experiments, where long background recording was maintained, the operator informed in advance about the time of sessions, etc. In the phase I of experiments, a nonlocal targeting ('address key') was not used (L=0 in Table II). All operators used only data graphs available in Internet. In the phase II (L=1), the operator drew a pattern by hand, it was cut into two halves, one half was mounted on a container with water, the second one was used by the operator. In the phase results of active sessions

N	time (D-M h:m)	ch1:Ψ	PRO	ch2:Ψ	PRO
1.	03-Jun 08:22:23	2.49	0.36	10.00	0.02
2.	05-Jun 03:34:46	-10.00	0.02	-0.53	0.98
3.	04-Jun 12:00:29	4.70	0.17	9.12	0.02
4.	02-Jun 21:18:35	2.03	0.50	8.23	0.05
5.	03-Jun 04:51:11	-8.11	0.03	-0.98	0.83
6.	03-Jun 17:55:18	-6.80	0.04	2.50	0.40
7.	05-Jun 02:34:28	-0.91	0.88	-6.39	0.04
8.	03-Jun 15:54:42	-5.94	0.04	1.55	0.57
9.	04-Jun 11:00:11	5.79	0.06	-0.82	0.94
10.	03-Jun 10:23:03	5.69	0.04	1.66	0.59
11.	03-Jun 18:25:27	-1.63	0.67	-5.61	0.06
12.	03-Jun 23:26:58	-5.54	0.12	-4.86	0.12
13.	03-Jun 08:52:34	1.00	0.91	-5.54	0.07
14.	04-Jun 05:58:46	-5.53	0.12	-2.89	0.35
15.	03-Jun 21:56:31	-5.42	0.10	-2.65	0.33
16.	04-Jun 21:03:00	-5.40	0.10	0.68	0.98
17.	03-Jun 14:54:24	5.24	0.06	-4.38	0.17
18.	04-Jun 23:03:32	-5.21	0.10	0.93	0.90
19.	05-Jun 01:34:12	1.01	0.83	5.20	0.04
20.	03-Jun 11:53:31	0.77	0.98	5.11	0.09
21.	03-Jun 12:23:40	3.33	0.15	5.04	0.11
22.	04-Jun 14:31:13	3.79	0.31	4.75	0.08
23.	03-Jun 03:20:41	-4.57	0.03	-1.79	0.62
24.	03-Jun 15:24:33	4.54	0.11	1.84	0.47
25.	05-Jun 07:05:44	0.75	0.96	-4.47	0.10
26.	04-Jun 01:27:32	-4.32	0.23	-2.84	0.29
27.	03-Jun 09:52:54	-0.68	0.96	4.24	0.11
28.	04-Jun 05:28:39	1.50	0.69	4.24	0.21
29.	04-Jun 04:58:31	0.55	1.00	-4.23	0.19
30.	03-Jun 18:55:36	4.22	0.17	1.24	0.75

A: mean Ψ of active sessions/mean Ψ of all sessions: 5.82/2.46=2.36
B: joint Probabil.Rand.Occur.(j-PRO): active ses./0.5 ses.: 2.82e-26
C: Mann-Whitney test (positive if < critical value): 0 (292 :1%, 338 :5%)

Figure 6. Evaluation of factors A, B, and C for the **maximal case** – the table of active sessions contains 30 maximum values sorted from all sessions for 3 days from a real EIS device.

III (L=2), photographic images were taken of water containers or sensors (as 'address keys' for instrumental experiments). From 34 attempts with operators (experiments 1-34), 25 were positive, which corresponds to 73.52% of the positive results. Since operators worked without training (or preparation), this result can be considered as the 'entry level'. Examples of EIS graphs and data from auxiliary sensors obtained in these experiments can be found in [44].

From those experiments we noted that: (1) the first session was the most intensive/successful; (2) the distance does not play any especial role, e.g., there is no difference in signals detected at distances of 3 km and 12000 km; (3) operators in phase I were not provided with address keys (images) – only data curves, available in Internet, however this was enough to generate a strong impact on sensors; (4) during the training process, the number of successful attempts increased, for example, in January's experiments of 2017, all attempts of one operator were successful; (5) operators carried the address keys all the time, also during emotionally intense events. However, we do not observe any particular changes in the dynamics at this time – apparently the concentration and altered state of consciousness are main elements for transmitting the distant impact.

Example of sessions 2018-2019. Active sessions were organized along the 'concentration', 'addressing' and 'intentions' training tasks with increasing complexity. Some operators use 'mental imagination' for targeting water samples, while others focus only on the online data plots.

Examples of sessions May-June and September 2019 are shown in Fig. 7 (one block with 30 active sessions requires about 1-2 months). We collect 31 (or 49) experiments for one

Table II
OVERVIEW OF EXPERIMENTS IN SEPTEMBER-JANUARY 2016-2017 (EXP. 35-39 ARE INSTRUMENTAL); OP. – OPERATOR, S – DISTANCE BETWEEN OPERATOR AND SENSORS, L – ADDRESSING METHOD (0 - WITHOUT EXPLICIT ADDRESSING, 1 – SYMBOL, 2 – IMAGE), k – RATIO OF EXPOSURE TIME TO DURATION OF BACKGROUND RECORDING; RES. – RESULT).

N	Op.	date	device	k	L	S,km	res.
1	O2	23.09.16,21.20-21.35	EIS:1	0.062	1	3	+
2	O2	24.09.16,06.00-6.30	EIS:1	0.111	1	3	-
3	O2	25.09.16,7.0-7.30	EIS:1	0.020	1	3	+
4	O2	25.09.16,21.50-22.10	EIS:1	0.023	1	590	+
5	O2	25.09.16,21.50-22.10	EIS:1	0.111	1	590	-
6	O2	26.09.16,23.50-0.15	EIS:1	0.095	1	610	+
7	O2	28.09.16,23.45-0.10	EIS:1	0.101	1	610	-
8	O2	6.10.16,8.30-10.00	EIS:3	0.022	1	1200	+
9	O2	7.10.16,17.00-17.30	EIS:3	0.014	1	1200	+
10	O2	8.10.16,10.57-11.28	EIS:3	0.071	1	1200	+
11	O2	8.10.16,12.30-13.30	EIS:3	0.071	1	1200	+
12	O1	7.12.16,7.00-7.20	phy:5	0.120	0	3	+
13	O1	14.12.16,5.00-5.30	EIS:3	0.111	0	3	- ()
14	O1	15.12.16,6.05-6.35	EIS:2.1	0.052	0	3	+
15	EG	15.12.16,17.00-17.30	phy:5	0.055	0	12000	+
16	O1	16.12.16,8.00-8.30	EIS:2.2	0.111	0	3	-
17	EG	17.12.16,9.08-10.00	EIS:2	0.111	0	12000	-
18	EG	17.12.16,10.32-11.20	EIS:3	0.076	0	12000	+
19	O1	17.12.16,10.19-10.45	phy:6	0.028	0	3	+
20	OP	17.12.16,21.45-22.25	phy:5	0.030	0	3	+
21	JP	17.12.16,23.30-0.40	EIS:2	0.089	0	>8500	+
22	JP	17.12.16,23.30-0.40	EIS:3	0.111	0	>8500	-
23	JP	17.12.16,23.30-0.40	phy:5	0.058	0	>8500	+
24	1+P	18.12.16,12.40-13.15	phy:7	0.111	0	3	-(e)
25	EG	18.12.16,12.57-14.00	EIS:3	0.111	0	12000	+
26	1+P	18.12.16,15.40-16.15	phy:6	0.142	0	3	+
27	YZ	19.12.16,15.30-15.50	EIS:3	0.045	0	>7500	+
28	EK	19.12.16,20.43-21.00	EIS:3	0.042	0	3	+
29	YZ	20.12.16,00.00-1.20	EIS:3	0.170	0	>7500	+
30	YZ	21.12.16,00.40-1.00	EIS:3	0.111	0	>7500	-
31	RY	21.12.16,21.00-22.00	EIS:3	0.100	0	>8500	+
32	O1	08.01.17,11.53-12.17	EIS:3		0	3	+
33	O1	9.01.17,23.50-01.20	EIS:2		0	3	+
34	O1	11.01.17,10.00-10.30	EIS:3		0	3	+
35	VZ	22.12.16,1.20-1.50	EIS:3	0.111	2	>2000	-
36	VZ	22.12.16,4.35-5.05	EIS:3.2	0.029	2	>2000	+
37	VZ	22.12.16,8.0-8.30	EIS:2.1	0.153	2	>2000	+
38	VZ	22.12.16,21.45-22.15	EIS:3,2	0.046	2	>2000	-
39	VZ	23.12.16,0.10-0.40	EIS:3,2	0.046	2	>2000	+

*() – full moon, *() – an electrically non-active plant

block of 30 (or 48) sessions, so that one session with lowest PRO value can be discarded from the table of results. This corresponds to the quota of 96.7% for 30 from 31 (and 97.9% for 48 from 49). Typically, there are about 50%-50% of original and post-sessions (18:12 in May-June, 14:16 in September). Half of all sessions is strong (PRO<0.25), about 3-4 sessions are on the mean level (0.6>PRO>0.4). We observe factors $A = 1.96, 1.91$ and $B = 10^{-20}, 10^{-19}$, which significantly differ from random values in Table I. The Mann-Whitney U test rejects the null hypothesis about the random nature of results. In other words, these data unambiguously confirm the effect of a distant influence on sensors, both in terms of the relationship between Ψ and Ψ_{mean}, as well as their statistical and probabilistic parameters.

Interesting high-level task in these sessions represents a 'distant transfer of intentions'. The EIS setup allows training results of active sessions

N	type	time (D-M h:m)	ch1:Ψ	PRO	ch2:Ψ	PRO
1.	1-post	28-Jun 09:00:11	2.09	0.42	9.55	0.02
2.	1-post	28-Jun 09:30:03	2.66	0.29	6.56	0.02
3.	1	06-Jun 08:30:00	-1.52	0.63	-6.11	0.04
4.	3	01-May 20:54:18	5.35	0.08	3.32	2.55
5.	2	23-Jun 23:23:54	-1.17	0.60	5.26	0.01
6.	1	24-Jun 20:00:16	-0.69	0.90	-5.25	0.07
7.	1-post	24-Jun 09:30:05	4.46	0.07	-4.62	0.09
8.	2	06-Jun 22:27:54	-2.52	0.26	-4.60	0.04
9.	1	29-May 08:30:01	4.21	0.06	2.77	0.37
10.	1-post	24-Jun 09:00:14	1.67	0.52	4.07	0.13
11.	1	01-Jul 08:30:13	3.99	0.23	-0.81	0.86
12.	3	10-May 08:30:01	-1.86	0.56	-3.94	0.21
13.	3	06-May 08:30:05	3.87	0.08	-1.18	0.16
14.	2	15-Jun 18:18:51	3.85	0.02	3.16	0.04
15.	2	05-Jun 22:35:15	2.75	0.09	3.75	0.09
16.	1-post	05-Jun 09:02:22	3.74	0.22	-2.27	0.41
17.	1	27-May 08:30:02	-2.00	0.22	-3.69	0.15
18.	1	07-May 08:30:06	2.36	0.30	3.55	0.20
19.	1-post	26-Jun 09:00:06	-1.64	0.54	3.36	0.28
20.	1	05-Jun 08:32:14	2.77	0.32	-3.29	0.26
21.	1-post	25-Jun 09:30:05	3.20	0.15	-2.39	0.33
22.	1	11-Jun 15:00:11	3.19	0.53	0.57	1.00
23.	1	25-Jun 08:30:06	0.53	1.00	3.14	0.19
24.	1-post	07-Jun 09:00:09	-0.81	0.68	3.01	0.18
25.	1	28-May 08:30:06	1.10	0.81	-2.94	0.40
26.	1	13-Jun 09:00:02	1.24	0.49	2.92	0.20
27.	1-post	07-Jun 09:30:01	1.59	0.39	-2.79	0.27
28.	1-post	13-Jun 09:30:12	-2.74	0.25	-2.63	0.24
29.	2-post	10-Jun 23:20:16	2.00	0.23	2.63	0.09
30.	1-post	13-Jun 10:00:04	2.58	0.26	2.19	0.32

A: mean Ψ of active sessions/mean Ψ of all sessions: 4.06/2.12=1.92, (1.96)
B: joint Probabil.Rand.Occur.(j-PRO): active ses./0.5 ses.: 4.12e-20
C: Mann-Whitney test (positive if < critical value): 12 (292 :1%, 338 :5%)

results of active sessions

N	type	time (D-M h:m)	ch1:Ψ	PRO	ch2:Ψ	PRO
1.	1	18-Sep 08:30	-5.20	0.02	1.26	0.64
2.	2	24-Sep 08:30	2.12	0.36	9.90	0.02
3.	4-post	19-Sep 09:30	6.54	0.02	0.74	1.00
4.	2-post	01-Oct 09:30	2.58	0.28	5.74	0.02
5.	1-post	12-Sep 09:30	-4.16	0.02	-2.30	0.18
6.	2-post	27-Sep 09:00	3.65	0.09	3.71	0.02
7.	4-post	20-Sep 09:30	7.34	0.03	4.65	0.11
8.	4	19-Sep 08:30	5.17	0.05	3.70	0.23
9.	1-post	13-Sep 09:00	5.35	0.07	-0.97	0.84
10.	2-post	26-Sep 08:59	4.52	0.07	5.31	0.10
11.	1-post	25-Jul 10:00	2.23	0.50	-4.02	0.08
12.	1-post	13-Sep 09:30	4.89	0.09	3.04	0.16
13.	1-post	17-Sep 09:30	-4.19	0.11	-1.98	0.61
14.	2-post	30-Sep 09:29	3.93	0.13	1.55	0.56
15.	1	12-Sep 08:30	2.37	0.15	-2.50	0.19
16.	2	27-Sep 08:30	-2.67	0.15	-2.48	0.18
17.	2	26-Sep 08:00	-0.69	0.98	-4.31	0.15
18.	1-post	16-Sep 09:30	-3.22	0.26	0.62	0.96
19.	2-post	25-Sep 09:00	-0.63	1.00	3.16	0.28
20.	2-post	25-Sep 09:30	2.46	0.36	-2.98	0.30
21.	2	20-Sep 08:30	3.02	0.30	-1.39	0.66
22.	4	20-Sep 08:30	3.02	0.30	-1.39	0.66
23.	2	01-Oct 08:30	-2.35	0.31	-1.47	0.58
24.	2-post	28-Sep 18:00	-2.39	0.36	1.39	0.74
25.	1-post	25-Jul 09:30	-3.13	0.42	1.75	0.46
26.	1	16-Sep 09:00	2.42	0.42	2.69	0.45
27.	2	30-Sep 08:30	-2.15	0.42	-1.14	0.78
28.	2	28-Sep 17:00	-0.71	0.98	2.34	0.45
29.	1	13-Sep 08:30	-0.70	0.98	-1.93	0.49
30.	2	25-Sep 08:30	1.25	0.78	1.32	0.62

A: mean Ψ of active sessions/mean Ψ of all sessions: 1.91
B: joint Probabil.Rand.Occur.(j-PRO): active ses./0.5 ses.: 4.82e-19
C: Mann-Whitney test (positive if < critical value): 80 (292 :1%, 338 :5%)

Figure 7. Examples of active sessions in May-June and September 2019 (public sensors), compare with the Table I.

this ability by transmitting the intentions of 'stimulation' and 'inhibition'. This is reflected as increasing or decreasing intensity of ionic dynamics and measured as an upward or downward trend after the regression. In the example in Fig. 8, an operator had two sessions of 10 minutes, separated by a pause of 30 minutes. In the first session, the '+' intention was transmitted that increases the electrochemical degradation and manifests as an upward trend. In the second session, the '-' intention was transmitted that reduces the electrochemical degradation and manifests as downward trend. These experiments allow removing any doubts about the influence of other factors – such a dynamics is almost impossible to create by accident, see [47].

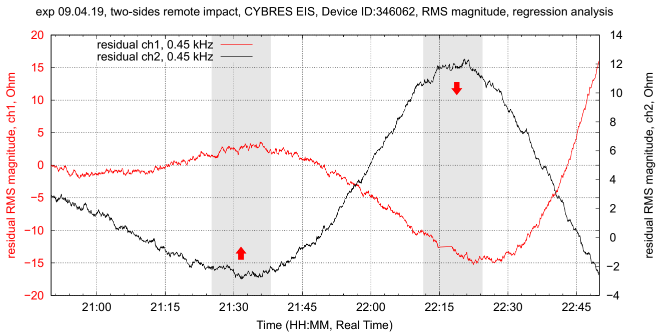

Figure 8. An example of training session on 'distant transfer of intention' – distant influence on electrochemical degradation, which manifests as an increase/decrease of trend in relation to the background recording.

Reiki practices. These sessions have been performed by operators who practice Reiki. One of Reikis main paradigms is that 'healing power' is not generated by operators, they only 'transmit it to patients' or even to technical devices [48]. As the operators describe, they followed such an approach, even without focusing on the EIS sensor. Figure 9 demonstrates results of active sessions performed with basic Reiki techniques in October-November 2019. The methodology, sensors and operators are the same as in May and September sessions, which are performed without Reiki. We observe 14 original and 16 post-sessions, 22 sessions have PRO < 0.25 that corresponds to 73% of all sessions (without Reiki it has about 55%). The factor $A = 2.27$ is about 20% higher than in September, and the factor $B = 10^{-21}$ is two orders of magnitude smaller, see

results of active sessions

N	type	time (D-M h:m)	ch1:Ψ	PRO	ch2:Ψ	PRO
1.	2-post	04-Oct 10:00	8.83	0.02	3.87	0.13
2.	1	05-Oct 16:30	9.90	0.02	3.09	0.22
3.	2-post	08-Nov 09:30	-1.92	0.42	-9.90	0.02
4.	2-post	06-Nov 09:00	4.37	0.09	9.90	0.02
5.	2-post	06-Nov 09:30	6.30	0.04	9.90	0.02
6.	2-post	17-Oct 09:00	-1.71	0.57	-6.11	0.02
7.	2	08-Nov 08:30	0.84	0.88	6.99	0.04
8.	2-post	04-Oct 09:29	2.69	0.20	-4.54	0.04
9.	2-post	08-Oct 09:00	5.50	0.04	-0.46	0.93
10.	2-post	07-Nov 09:00	-3.31	0.19	4.53	0.06
11.	2-post	11-Oct 09:30	7.64	0.06	0.62	0.91
12.	2-post	04-Nov 09:00	4.52	0.06	3.34	0.35
13.	2	09-Oct 08:30	-3.27	0.24	-3.43	0.09
14.	2	15-Oct 08:30	1.58	0.60	3.77	0.09
15.	2	11-Nov 08:30	-3.15	0.17	-3.96	0.11
16.	2	08-Oct 08:30	4.13	0.15	-1.17	0.72
17.	2	17-Oct 08:30	3.83	0.17	1.54	0.63
18.	2-post	11-Oct 09:00	1.25	0.74	5.27	0.17
19.	2-post	11-Oct 09:00	1.25	0.74	5.27	0.17
20.	2	21-Oct 08:30	4.29	0.20	-1.76	0.56
21.	2	04-Nov 08:30	-0.71	0.96	-4.68	0.20
22.	2	16-Oct 08:30	1.44	0.60	-3.51	0.21
23.	2-post	10-Oct 10:00	-1.71	0.50	-4.18	0.26
24.	2	04-Oct 09:00	2.34	0.28	-2.29	0.38
25.	2-post	22-Oct 09:00	-0.95	0.81	-2.80	0.30
26.	2-post	23-Oct 09:00	-2.96	0.31	1.82	0.59
27.	2	11-Oct 08:30	1.25	0.74	3.06	0.37
28.	2	23-Oct 08:30	-0.52	1.00	-2.62	0.38
29.	2-post	10-Oct 09:30	2.22	0.39	2.10	0.59
30.	2	22-Oct 08:30	2.42	0.44	-1.43	0.70

A: mean Ψ of active sessions/mean Ψ of all sessions: 2.27
B: joint Probabil.Rand.Occur.(j-PRO): active ses./0.5 ses.: 1.60e-21
C: Mann-Whitney test (positive if < critical value): 54 (292 :1%, 338 :5%)

Figure 9. Results of distant Reiki sessions in October-November 2019.

Table I – thus, the results of active sessions are stronger even if using only basic Reiki elements.

A. Analysis of EEG and EIS data

Involving the EEG feedback in training process allows more accurately determining various mental states of operators and comparing them with results of distant sessions. EEG sensors provide data before (in the relaxation phase) and during the session, thus, it allows evaluating, for example, readiness of operators and used strategies for remote actions. The relationship between EEG and meditative states has been investigated many times, see e.g. [49], [50]. In general, the topic of neurocognitive feedback with EEG and EIS deserves a separate work, here we briefly mention only two points: the difference between remote sessions and meditative practices, and the 'minimal threshold of effort' required to generate a distant impact.

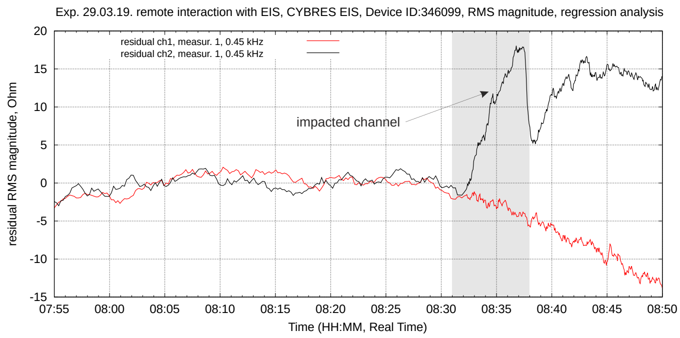

(a)

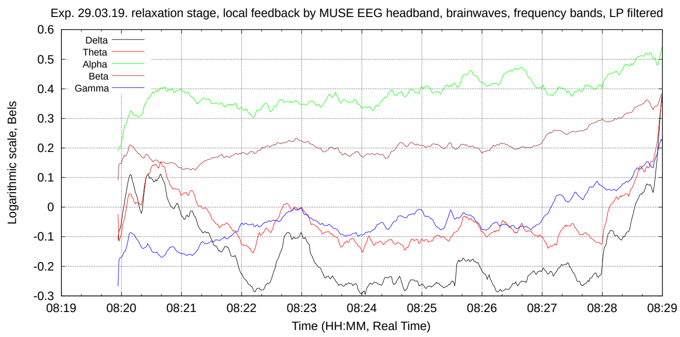

(b)

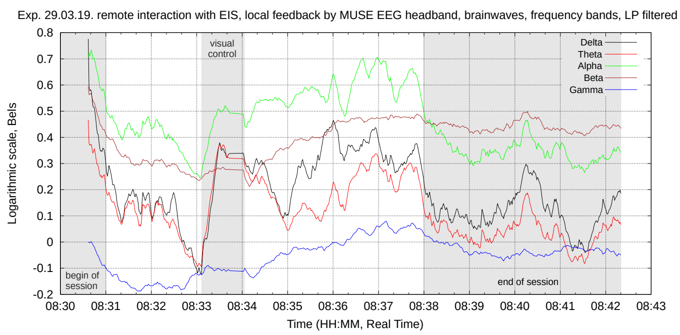

(c)

Figure 10. An example of distant influence with EIS and EEG data before the session (relaxation phase) and during the session. **(a)** EIS data in the background and experimental regions, linear regression, channel 1 was affected; **(b)** EEG data in the relaxation phase; **(c)** EEG data in the active phase.

Active vs relaxation meditation. Fig. 10 shows a session with distant influence on channel 1, which was preceded by a 10-minute relaxation phase. A typical characteristic of relaxation and meditation states is an increased alpha activity and calm dynamics of all other rhythms. In a normal state of consciousness with open eyes, the rhythms mix, the beta component increases. These conditions are observed in this experiment, both in the phase of relaxation and during the session when the operator opened his eyes for a visual control of data. The active session has a combination of high alpha and delta rhythms with the excited dynamics of other components. A characteristic point is '8:38' – at this moment we observe a correlation between the EEG and the EIS data – a jump in the EIS curve of channel 1 and a change in the alpha, delta and theta rhythms. This is consistent with the description of operators who compare remote sessions with an 'active meditation', as opposed to 'passive meditation' in typical meditative states.

Here we can express a hypothesis, which was also observed in earlier experiments [6], [43], – relaxation states do not contribute to distant effects. Remote sessions require a high 'mental activity', but in an altered state of consciousness, as indicated by a high alpha rhythm. We refer such states as 'active meditation' (AM).

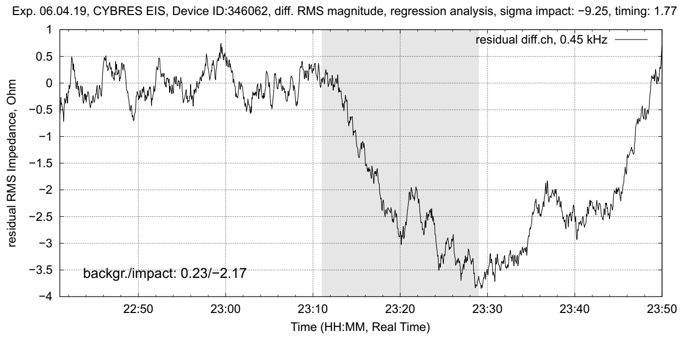

(a)

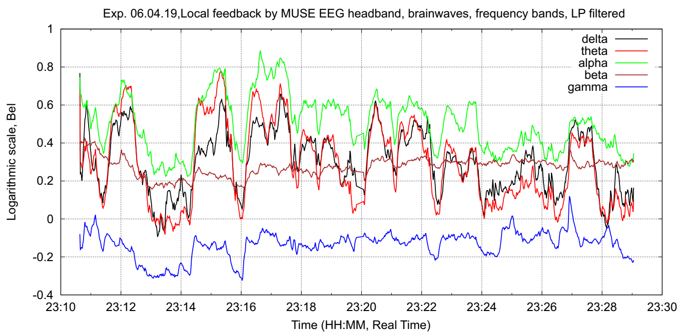

(b)

Figure 11. An example of an experiment to determine the minimum threshold of mental effort to generate distant influence. **(a)** EEG data; **(b)** EIS data.

Minimal threshold of efforts. An important research question is related to the so-called 'minimal threshold' – the minimal level of mental efforts required to create a detectable change in EIS dynamics. In these tests, operators are encouraged to avoid relaxing, deep or active meditation and conduct a remote session in a state close to normal. To some extent, these experiments mimic the ability of operators to produce distant effects in everyday situations (e.g. emotional events) without any preparatory steps. These attempts are made regularly, and changes in the 'minimal threshold' indicate a progress in training. For example, during the initial attempts, we did not register any measurable distant effects without entering into the AM state.

Typical EEG diagrams of these tests do not include preparatory relaxation phases and record only the remote sessions, see Fig. 11. Here we observe usual patterns of alpha, delta, and theta rhythms that are characteristic of the 'active brain' stage. However, the increased alpha and low beta components are unusual in this experiment, which may indicate that the operator is in a shallow altered state of consciousness. EIS sensors demonstrate a high result ($\Psi > 5$), where the trend changes immediately after the session. This experiment shows an interesting feature of trained operators to enter altered states of consciousness, and, accordingly, the ability to remote actions during everyday activities (which may be considered as one of goals for the training).

V. Conclusion

This paper reported about a new methodological approach of using bio-feedback in training unusual operator capabilities. Two feedback loops with local EEG sensors and distant EIS systems provide in real time objective measure of distant activities and metal states during active sessions. In total, several hundred distant experiments between 2015 and 2019, in blocks of 30 sessions, have been performed, for which statistical and probabilistic parameters are calculated. Distance in local experiments varies between 10-20 meters (in different laboratories) and 3-5 km, in global experiments – 10^3-10^6 meters. Typical results of 39 active sessions are summarized in Table II for early attempts 2017-2018 and in Table I and Fig. 7 for 90 attempts in 2019. For comparison, 90 passive sessions (control experiments) are collected in different conditions, they enable evaluating boundary values of parameters A, B and C.

Improvements of measuring system, methodology and training of operators contributed to increasing a success rate of these attempts: from 74% in 2016-2017 up to 96% in 2019. We observe a clear difference in factors A and B between random EIS data and results of real sessions. The Mann-Whitney test also rejected the null hypothesis for real sessions. Thus, in a large amount of statistically significant data we observe multiple evidences of disturbances of electrochemical dynamics that are strongly correlated with time of distant attempts.

Beside experiments with operators, continuously running sensors record environmental fluctuations that are correlated with some global events. Example of global fluctuations is shown in Fig. 12 that demonstrates the standard deviation in B-area for June 2019, averaged in a sliding window of 24 hours. Two peaks on these graphs on both EIS channels coincide with the full moon and the summer solstice on June 17 and June 21.

To generalize, this work described the methodology of sensors data processing that enables well-repeatable measurement of ultra-weak influences on electrochemical dynamics of aqueous solutions. The methodology of experiments can be utilized not only for assessing distant activities of human operators, but also for measuring environmental influences, technological or infoceutical effects. It was shown that a significant improvement of operator's results and extensions of methodology are possible in the process of training. In addition, many interesting scientific aspects of systems with EEG and EIS feedback remained open: biophysics, psychosomatics, brain-computer interface, long-range signal transmission, quantum phenomena in biological systems – which represent a large technological area and focuses of further experiments.

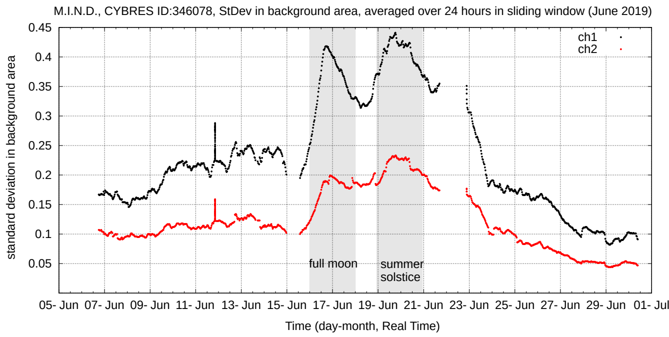

Figure 12. MIND sensor without public access, June 2019, shown is the standard deviation in background region, averaged in a sliding window of 24 hours. The first peak coincides with the full moon on June 17 and the second peak on June 21 – with the summer solstice.

References

[1] L.L. Vasiliev. *Experiments in Distant Influence*. Wildwood House Ltd, 1976.

[2] V.P. Perov. Investigating the coupling between sensorial-disconnected bio-objects (rus). *In Proc.: Krasnogorskaj N.V. (ed.). Electromagnetic fields in biosphere*, (N1):362, 1984.

[3] A.E. Akimov, V.J. Tarasenko, and S.U. Tolmachev. Torsion communication – new system for telecommunication (rus). *Electrocommunication (Electrosvjz)*, (5), 2001.

[4] Patrice K. Pasturel G. Scott Hubbard, Philip P. Bentley. *A remote action experiment with a piezoelectric transducer*. CIA-RDP96-00787R000300300001-7, 1987.

[5] Edwin C. May, Victor Rubel, and Loyd Auerbach. *ESP WARS: East and West: An Account of the Military Use of Psychic Espionage As Narrated by the Key Russian and American Players*. CreateSpace Independent Publishing Platform, 2014.

[6] Serge Kernbach, Vitaliy Zamsha, and Yuri Kravchenko. Experimental approach towards long-range interactions from 1.6 to 13798 km distances in bio-hybrid systems. *NeuroQuantology*, 14(3):456–476, 2016.

[7] A.V. Bobrov. *Investigating a field concept of consciousness (rus)*. Orel, Orel University Publishing, 2006.

[8] V.A. Sokolova. *First experimental confirmation of torsion fields and their usage in agriculture (rus)*. Moscow, 2002.

[9] S.Zenin. *Structured state of water as a basis for monitoring of living systems (rus)*. M.: PGB, 2005.

[10] Serge Kernbach. Replication attempt: Measuring water conductivity with polarized electrodes. *Journal of Scientific Exploration*, 27(1):69–105, 2013.

[11] Serge Kernbach and Olga Kernbach. Impact of structural elements on high frequency non-contact conductometry. *IJUS*, 12-13(4):47–68, 2016.

[12] S. Kernbach, I. Kuksin, and O. Kernbach. Analysis of ultraweak interactions by electrochemical impedance spectroscopy (rus). *IJUS*, 11(4):6–22, 2016.

[13] S. Kernbach. *Supernatural. Scientifically proven facts (rus)*. Algorithm. Moscow, 2015.

[14] B.K. Ratnikov and G.G. Rogozin. *Image of world in representation of special services (rus)*. The control academy, 2011.

[15] N.A.Sham. *Clairvoyants in the service of the KGB (interview, rus)*. 'Moskovsky Komsomolets' N27745 of August 1, 2018, 2018.

[16] N. Poroskov. *Super Soldier for Future Wars (rus)*. 'Armeyskij Sbornik', Journal of the Ministry of Defense of the Russian Federation, N2, p. 86-90, February 26, 2019.

[17] Tom Parfitt. *Russian military claims psychic powers*. The Times, April 5, 2019, 26.02.2019.

[18] Sheng-Ping Li, Gui-Rong Meng, Meng-Yin Sun, and et al. Experimental research of the influence of qigong external qi on the material molecule (chinese). *The Journal of Nature*, 10:52–57+82, 1988.

[19] Xin Yan, Zu-Yin Lu, and En-Shen Yan. Observation of the influence of qigong external qi on the laser polarization plane (chinese). *International Medical Qigong Academic Conference*, 10:52–57+82, 1988.

[20] Xin Yan, Sheng-Ping Li, Jian-Yuan Yu, and et al. Observation of the influence of qigong external qi on the solution with physiological effect measured by laser raman spectroscopy[j](chinese). *The Journal of Nature*, 08, 1988.

[21] V.Vedral. *Decoding Reality: The Universe as Quantum Information*. Oxford, 2010.

[22] J. Sperling and I. A. Walmsley. Entanglement in macroscopic systems. *Phys. Rev. A*, 95:062116, Jun 2017.

[23] T. A. Palomaki, J. D. Teufel, R. W. Simmonds, and K. W. Lehnert. Entangling mechanical motion with microwave fields. *Science*, 342(6159):710–713, 2013.

[24] Mei Wang, Xin-You Lü, Ying-Dan Wang, J. Q. You, and Ying Wu. Macroscopic quantum entanglement in modulated optomechanics. *Phys. Rev. A*, 94:053807, Nov 2016.

[25] C. F. Ockeloen-Korppi, E. Damskagg, J.-M. Pirkkalainen, A. A. Clerk, F. Massel, M. J. Woolley, and M. A. Sillanpaa. Stabilized entanglement of massive mechanical oscillators. *Nature*, 556:062116, 2018.

[26] Serge Kernbach. Distant monitoring of entangled macro-objects. *NeuroQuantology*, 17(3):16–39, 2019.

[27] Lee-Fan Tan, Ashok Jansari, Shian-Ling Keng, and Sing-Yau Goh. Effect of mental training on bci performance. In Julie A. Jacko, editor, *Human-Computer Interaction. Novel Interaction Methods and Techniques*, pages 632–635, Berlin, Heidelberg, 2009. Springer Berlin Heidelberg.

[28] Khaled Hegazy. *The Effect of Mental Training on Precision Tasks in Tennis and Soccer: a Study on Educational Technology*. PhD thesis, Universitat Konstanz, Konstanz, 2012.

[29] Michael Burger. *Sources for the History of Western Civilization: From Antiquity to the Mid-Eighteenth Century*. University of Toronto Press, 2015.

[30] R. Janhn, B. Dunne, G. Bradish, Y. Dobyns, A. Lettieri, R. Nelson, J. Mischo, E. Boller, H. Boesch, D. Vaitl, J. Houtkooper, and B. Walter. Mind/machine interaction consortium: PortREG replication experiments. *Journal of Scientific Exploration*, (14(4)):499–555, 2000.

[31] Ingo Swann. *Natural ESP*. Bantam, 1987.

[32] G.N. Dulnev and A.P. Ipatov. *Investigation of energo-information exchange: experimental results (rus)*. GITMO, S-Petersburg, 1998.

[33] St. LaBerge and H Rheingold. *Exploring the World of Lucid Dreaming*. Ballantine Books, 1991.

[34] D.D.O. Oyebola. The method of training traditional healers and midwives among the yoruba of nigeria. *Social Science & Medicine. Part A: Medical Psychology & Medical Sociology*, 14(1):31 – 37, 1980.

[35] Sheffy Bhayee, Patricia Tomaszewski, Daniel Lee, Graeme Moffat, Lou Pino, Sylvain Moreno, and Norman Farb. Attentional and affective consequences of technology supported mindfulness training: A randomised, active control, efficacy trial. *BMC Psychology*, 4, 12 2016.

[36] Natasha Kovacevic, Petra Ritter, William Tays, Sylvain Moreno, and Anthony Randal McIntosh. My Virtual Dream: Collective neurofeedback in an immersive art environment. *PLoS One*, 10(7), 2015.

[37] H. Alvin Sharpe. *Collective Meditations*. Dixie Savers Club, 1979.

[38] S. Kernbach, I. Kuksin, O. Kernbach, and A. Kernbach. The vernadsky scale – on metrology of EIS in time-frequency domain. *IJUS*, 143–150(5):62–87, 2017.

[39] S. Kernbach. Distant monitoring of entangled macro-objects. *NeuroQuantology*, 17(3):19–4, 2019.

[40] S. Kernbach and O. Kernbach. On precise *pH* and *dpH* measurements (rus). *International Journal of Unconventional Science*, 5(2):83–103, 2014.

[41] S. Kernbach, I. Kuksin, and O. Kernbach. On accurate differential measurements with electrochemical impedance spectroscopy. *WATER*, 8:136–155, 2017.

[42] CYBRES. *Application Note 26. Methodology and protocols of feedback-based EIS experiments in real time*. 2019.

[43] S. Kernbach, V. Zamsha, and Y. Kravchenko. Long and super-long range device-device and operator-device interactions. *International Journal of Unconventional Science*, 1(1):24–42, 2013.

[44] CYBRES. *Application Note 18 'Online system for automatic detection of remote interactions based on the CYBRES MU EIS impedance spectrometer'*. 2017.

[45] S.Kernbach and O.Kernbach. Distant effects of Reiki (rus). *IJUS*, 25-26(7):38–48, 2020.

[46] J.E. Dennis and R.B. Schnabel. *Numerical methods for unconstrained optimization and nonlinear equations*. Prentice-Hall Series in Computational Mathematics, Englewood Cliffs, 1983.

[47] S.Kernbach and O.Kernbach. On temporal anomalies in macro-quantum interactions (rus). *IJUS*, 23-24(7):90–102, 2019.

[48] Brett Bevell. *The Reiki Magic Guide to Self-Attunement*. Crossing Press, 2007.

[49] Juergen Fell, Nikolai Axmacher, and Sven Haupt. From alpha to gamma: Electrophysiological correlates of meditation-related states of consciousness. *Medical hypotheses*, 75:218–24, 03 2010.

[50] Aviva Berkovich-Ohana, Joseph Glicksohn, and Abraham Goldstein. Mindfulness-induced changes in gamma band activityimplications for the default mode network, self-reference and attention. *Clinical neurophysiology : official journal of the International Federation of Clinical Neurophysiology*, 123:700–710, 09 2012.